Review of Last Lecture

$$J_{ex} = L_{11}\left(-\frac{d\Phi}{dx}\right) + L_{12}\left(-\frac{dT}{dx}\right) \qquad J_{qx} = L_{21}\left(-\frac{d\Phi}{dx}\right) + L_{22}\left(-\frac{dT}{dx}\right)$$

Onsager Relation: $L_{21}=TL_{12}$

$$L_{11} = \sigma = -\frac{e^2}{3}\int v^2 \tau \frac{\partial f_o}{\partial E} D(E)dE$$

$$L_{12} = \frac{e}{3T}\int v^2\tau(E - E_f)\frac{\partial f_o}{\partial E} D(E)dE$$

$$L_{22} = -\frac{1}{3T}\int (E - E_f)^2 v^2\tau\frac{\partial f_o}{\partial E} D(E)dE$$

Property Examples

Images removed due to copyright restrictions.
Please see Fig. 2a, b in Poudel, Bed, et al.
"High-Thermoelectric Performance of Nanostructured Bismuth Antimony Telluride Bulk Alloys." *Science* 320 (May 2, 2008): 634-638.

$$\sigma = \frac{e^2}{3}\int \tau \mathbf{v}^2 \mathrm{D(E)}(-\partial f_{eq}/\partial \mathrm{E})\mathrm{dE}$$

$$\propto \left(\mathrm{k_B}T\right)^{\gamma+3/2} \exp\left(-\frac{E_c-\mu}{k_B T}\right)$$

For nondegenerate semiconductor only

- **Optimal thermoelectric materials are usually degenerate**
- **Multiband transport important at high temperatures, leading to decreasing Seebeck coefficient with increasing temperature**

Phonon Heat Conduction

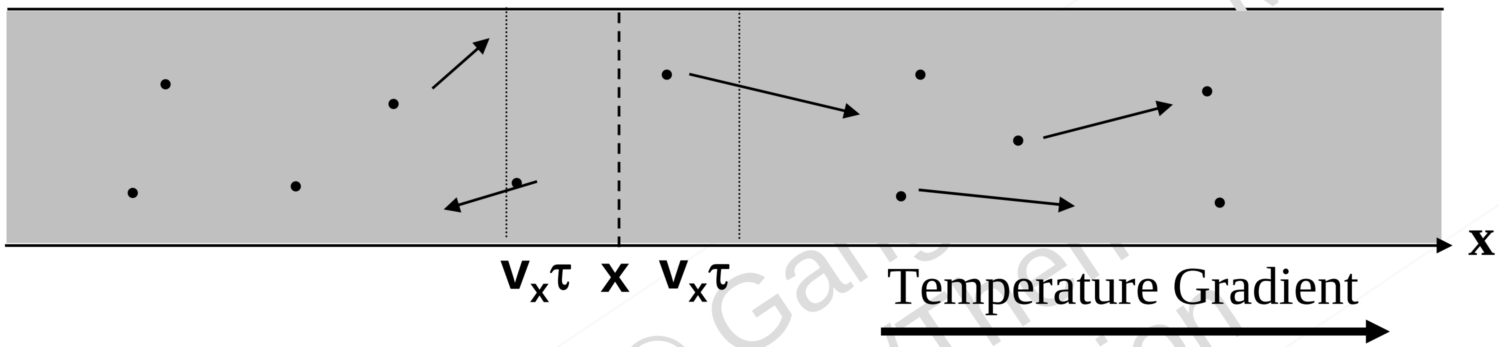

$$q_x = \frac{1}{2}\sum_{k_x}\sum_{k_y}\sum_{k_z}\left[\hbar\omega f(T)v_x\right]\Big|_{x-v_x\tau} - \sum_{k_x}\sum_{k_y}\sum_{k_z}\left[\hbar\omega f(T)v_x\right]\Big|_{x+v_x\tau}$$

$$= -k\frac{dT}{dx}$$

where

$$k = \frac{1}{3}\int_0^{\omega_{\max}} v^2\tau\hbar\omega\frac{\partial f}{\partial T}D(\omega)d\omega$$

$$= \frac{1}{3}\int_0^{\omega_{\max}} C(\omega)v(\omega)\Lambda(\omega)d\omega$$

Typical Behavior of Phonon Thermal Conductivity

Boundary Scattering Dominant $k \sim T^3$

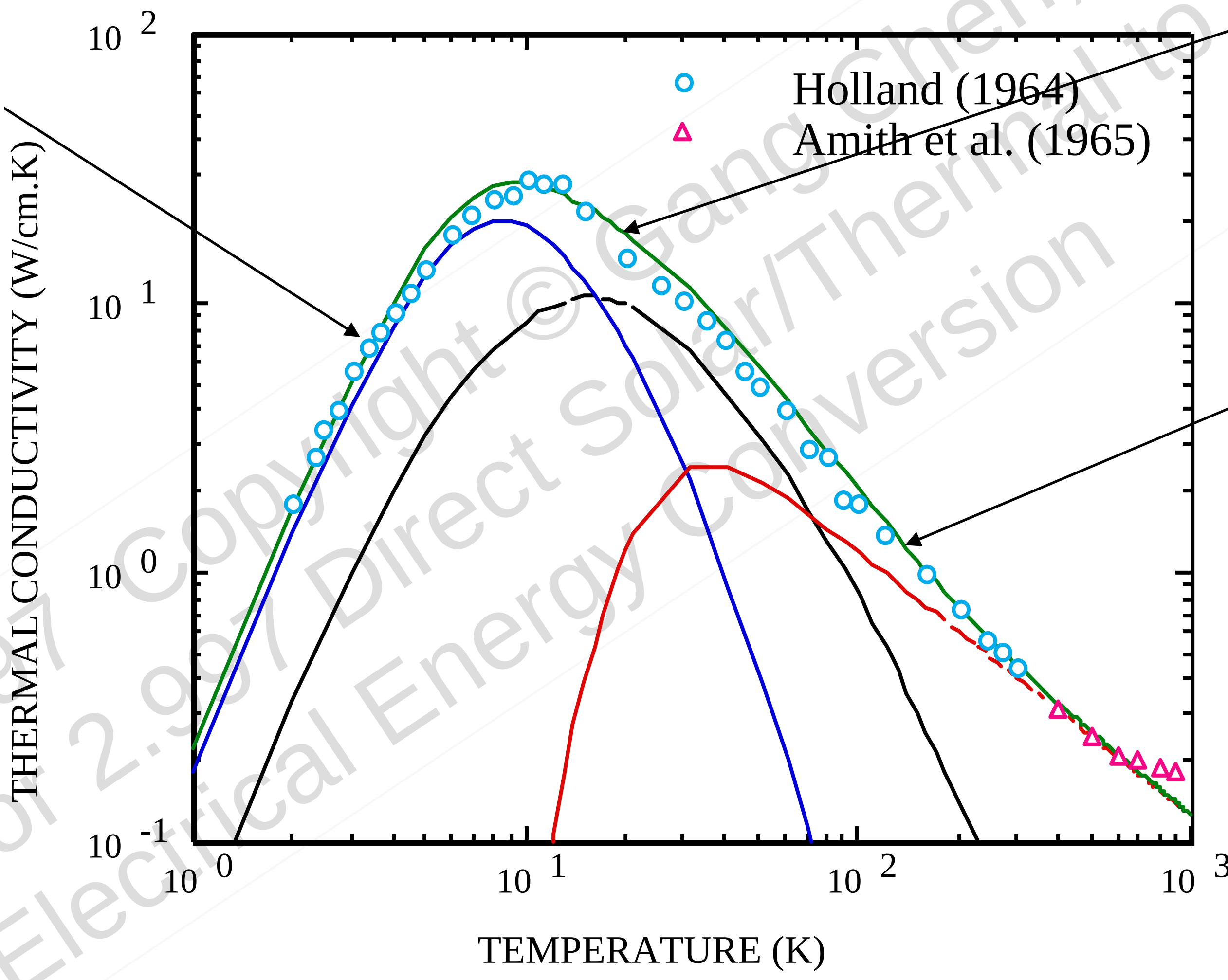

Impurity Scattering Dominant

Phonon-Phonon Scattering Dominant $k \sim 1/T^n$, n=1-1.5

Combined Electronic and Phononic Thermal Conductivity

$$k = k_L + k_a + k_b + (S_a - S_b)^2 T \frac{\sigma_a \sigma_b}{\sigma_a + \sigma_b}$$

Bipolar Contribution

Image removed due to copyright restrictions.
Please see Fig. 4 in Poudel, Bed, et al. "High-Thermoelectric Performance of Nanostructured Bismuth Antimony Telluride Bulk Alloys." *Science* 320 (May 2, 2008): 634-638.

Thermoelectric Figure of Merit

$$ZT = \frac{\sigma S^2 T}{k_e + k_p} = \frac{S^2}{\frac{k_e}{\sigma T} + \frac{k_p}{\sigma T}} = \frac{S^2}{L + \frac{k_p}{\sigma T}}$$

$$L = L(n) \approx 2.45x10^{-8}$$

In Metal, S~10 μV/K $\frac{k_p}{\sigma T} \leq L$ **ZT~0.01**

Good Thermoelectric Materials

S~200 μV/K,
k_p~1 W/mK,
σ~10^5 S/m

$$ZT = \frac{4\times 10^{-8}}{2.45\times 10^{-8} + 3\times 10^{-8}} \sim 1$$

Properties vs. Carrier Density

Image removed due to copyright restrictions.
Please see Fig. 3 in Minnich, A. J., et al.
"Bulknanostructured Thermoelectric Materials: Current Research and Future Prospects." *Energy and Environmental Science* 2 (2009): 466-479.

Classical Thermoelectric Materials

Material ZT

Image removed due to copyright restrictions.
Please see Fig. 1 in Minnich, A. J., et al.
"Bulk Nanostructured Thermoelectric Materials: Current
Rresearch and Future Prospects." *Energy and Environmental Science* 2 (2009): 466-479.

Minnich et al., Energy and Environmental Sci., Aug. 2009

P-type and N-type

Image removed due to copyright restrictions.
Please see Fig. B2a,b in Snyder, G. Jeffrey, and Eric S. Toberer.
"Complex Thermoelectric Materials." *Nature Materials* 7
(February 2008): 105-114.

Why Heavier Crystals?

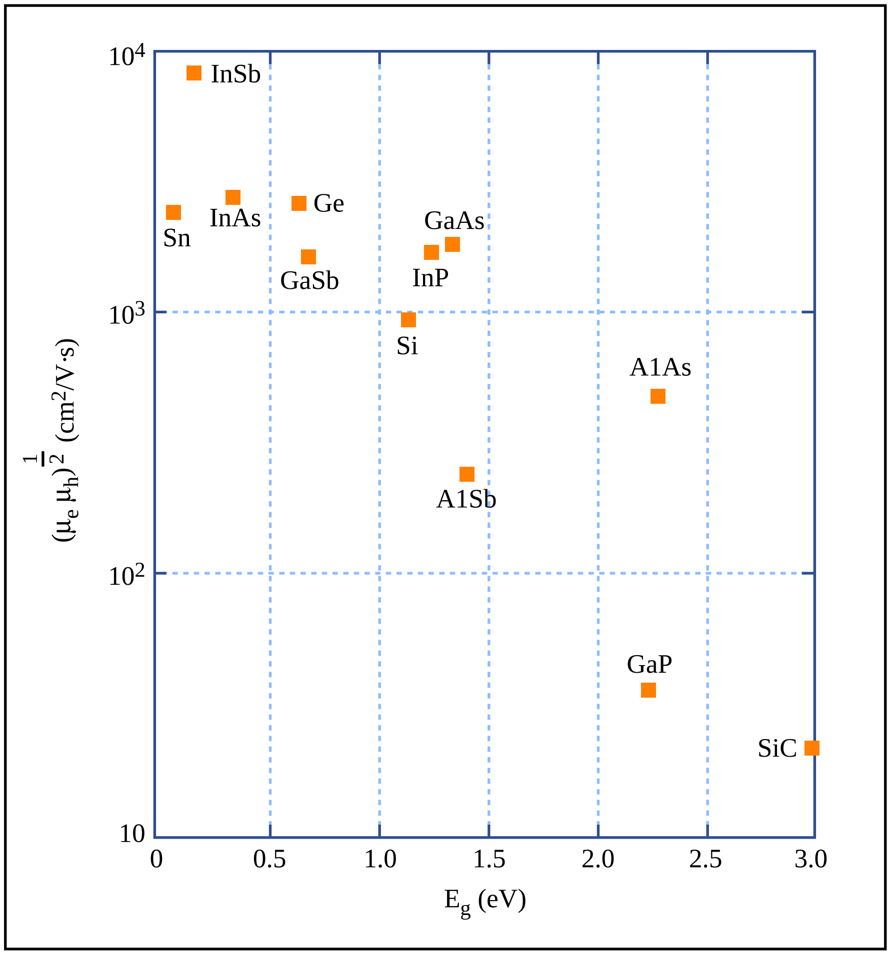

Figure by MIT OpenCourseWare.

- **Better mobility**
- **Lower phonon thermal conductivity**

From H.J. Goldsmid

Unit Cell

Image removed due to copyright restrictions.
Please see Fig. 1 (left) in Huang, Bao-Ling, and Massoud Kaviany.
"*Ab initio* and Molecular Dynamics Predictions for Electron and Phonon Transport in Bismuth Telluride." *Physical Review B* 77 (2008): 125209.

Huang and Kaviany, PRB, 77, 125209 (2008)

$$-Te^{(1)}]-[Te^{(1)}-Bi-Te^{(2)}-Bi-Te^{(1)}]-[Te^{(1)}-Bi-Te^{(2)}-Bi-Te^{(1)}]-[Te^{(1)}-$$

Electronic Band Structure

Images removed due to copyright restrictions.

Please see: Fig. 1 (right) in Huang, Bao-Ling, and Massoud Kaviany. "*Ab initio* and Molecular Dynamics Predictions for Electron and Phonon Transport in Bismuth Telluride." *Physical Review B* 77 (2008): 125209.

Fig. 4a in Larson, P., S. D. Mahanti, and M. G. Kanatzidis. "Electronic Structure and Transport of Bi2Te3 and BaBiTe3." *Physical Review B* 61 (March 2000): 8162-8171.

Larson et al., PRB, 61, 8261 (2000)

Figure of Merit

Image removed due to copyright restrictions.
Please see Fig. 16 in Huang, Bao-Ling, and Massoud Kaviany.
"*Ab initio* and Molecular Dynamics Predictions for Electron and
Phonon Transport in Bismuth Telluride." *Physical Review B* 77 (2008): 125209.

SiGe Alloys

- Abeles Virtual Crystal Model

Image removed due to copyright restrictions.
Please see Fig. 2 in Abeles, B. "Lattice Thermal Conductivity of Disordered Semiconductor Alloys at High Temperatures." *Physical Review* 131 (September 1963): 1906-1911.

Rayleigh Scattering

$$\tau_p^{-1} = \frac{\omega^4 \delta^3 \Gamma}{4\pi v^3}$$

Disorder Parameter

$$\Gamma = x(1-x)\left[\left(\frac{\Delta M}{M}\right)^2 + \varepsilon\left(\frac{\Delta \delta}{\delta}\right)^2\right]$$

Commercial Materials

- P-type: $Bi_{2-x}Sb_xTe_3$
- N-type: $Bi_2Sb_{3-x}Se_x$
- Doping mainly by defects
  - antisites, vacancies

Oxides

Images removed due to copyright restrictions.
Please see Fig. 2, 3 in Koumoto, Kunihito, Ichiro Terasaki, and Ryoji Funahashi. "Complex Oxide Materials for Potential Thermoelectric Applications." *MRS Bulletin* 31 (March 2006): 206-210.

Half Heusler

Image removed due to copyright restrictions.
Please see Fig. 4 in Nolas, George S., Joe Poon, and Mercouri Kanatzidis. "Recent Developments in Bulk Thermoelectric Materials." *MRS Bulletin* 31 (March 2006): 199-205.

Other Bulk Materials

Image removed due to copyright restrictions.
Please see Fig. 2 in Snyder, G. Jeffrey, and Eric S. Toberer.
"Complex Thermoelectric Materials." *Nature Materials* 7
(February 2008): 105-114.

All Classical Materials Used Alloy Scattering

- Bi_2Te_3 with Sb_2Te_3 and Bi_2Se_3
- PbTe with PbSe
- Si with Ge

Institutional Method

Structure

Formula TPn_3
T = transition metal (Co,Ir,Rh,Fe,Ni)
Pn = pnicogen (P,As,Sb)
space group Im$\bar{3}$
8 formula units/cell

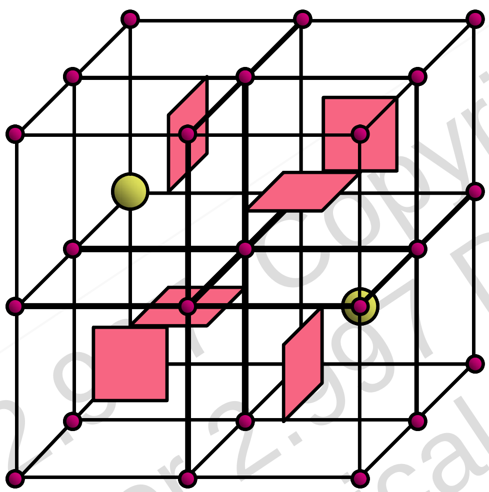

Properties

@ 300K	p-$CoSb_3$	p-$IrSb_3$
S [μV/K]	138	72
μ_{Hall} [cm^2/V-s]	1944	1320
p [cm^{-3}]	4.4 10^{18}	1.1×10^{19}
ρ [mΩ-cm]	0.74	0.44
κ [W/m-K]	11.8	16.0
optical gap [eV]	0.5	1.4
a_0 [nm]	0.9034	0.9250

References

J-P Fleurial, T. Caillat and A. Borshchevsky, AIP Press, 40-44 (1995); J.-P. Fleurial, A. Borshchevsky, T. Caillat, D. Morelli and G. P. Meisner, 15th International Conf. on Thermoelectrics (1996) 91-95; G. A. Slack and V.G. Tsoukala, J. Appl. Phys. 76 (1994) 1665.

Phonon Rattlers

Images removed due to copyright restrictions.
Please see Fig. 3, 4, 6 in Sales, B. C., et al.
"Filled Skutterudite Antimonides: Electron Crystals and Phonon Glasses."
Physical Review B 56 (December 1997): 15081-15089

Nanostructuring

Nanoscale Effects for Thermoelectrics

Interfaces that Scatter Phonons but not Electrons

Electrons
Λ=10-100 nm
λ=10-50 nm

Phonons
Λ=10-100 nm
λ=1 nm

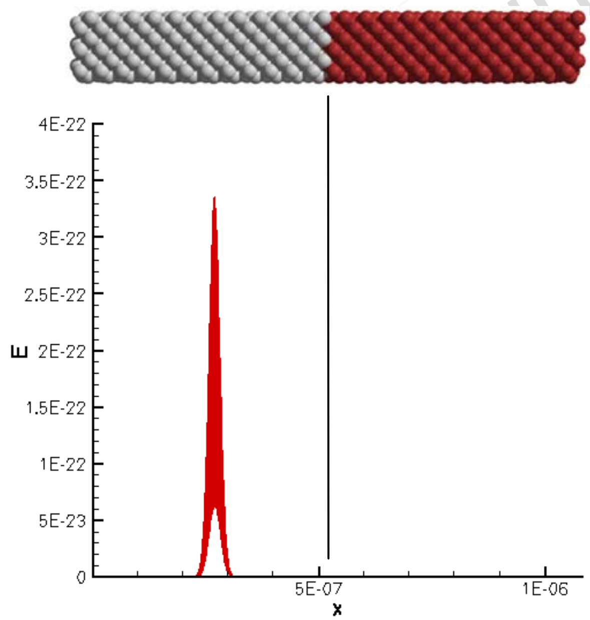

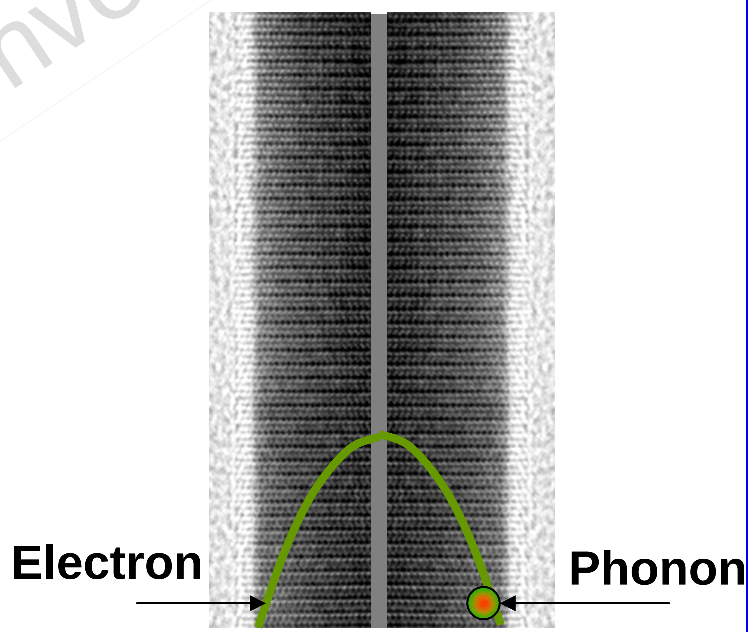

Superlattice Structures with Enhanced ZT

PbTe/PbTeSe Quantum Dot Superlattices

Ternary: ZT=1.3-1.6
Quaternary: ZT=2
ΔT=43.7 K, Bulk ΔT=30.8 K
T.C. Harman, Science, 2002

ΔT=32.2 K, ZT ~2-2.4
R. Venkatasubramanian, Nature, 2001

PbTe/PbSeTe	Nanostructure	Bulk	Bi_2Te_3/Sb_2Te_3	Superlattice	Bulk
Power Factor ($\mu W/cmK^2$)	32	28		40	50.9
Conductivity (W/mK)	0.6	2.5		0.5	1.26

Heat Conduction Mechanisms in Superlattices

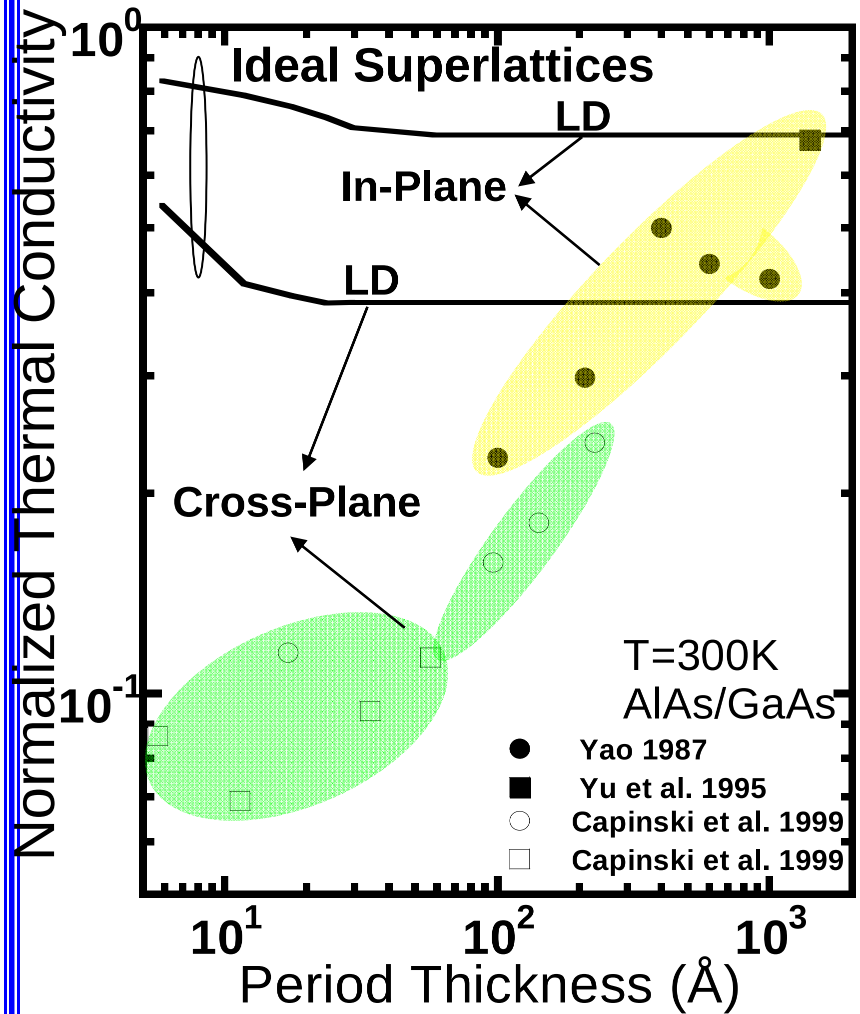

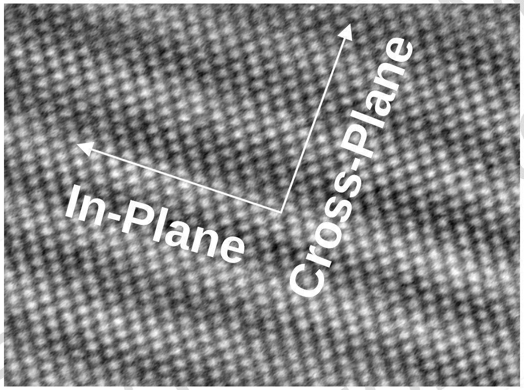

Major Conclusions:

- **Ideal superlattices do not cut off all phonons due to pass-bands**
- **Individual interface reflection is more effective**
- **Diffuse phonon interface scattering is crucial**

Periodic Structures Are Not Necessary, Nor Optimal!

Nanocomposites Approach

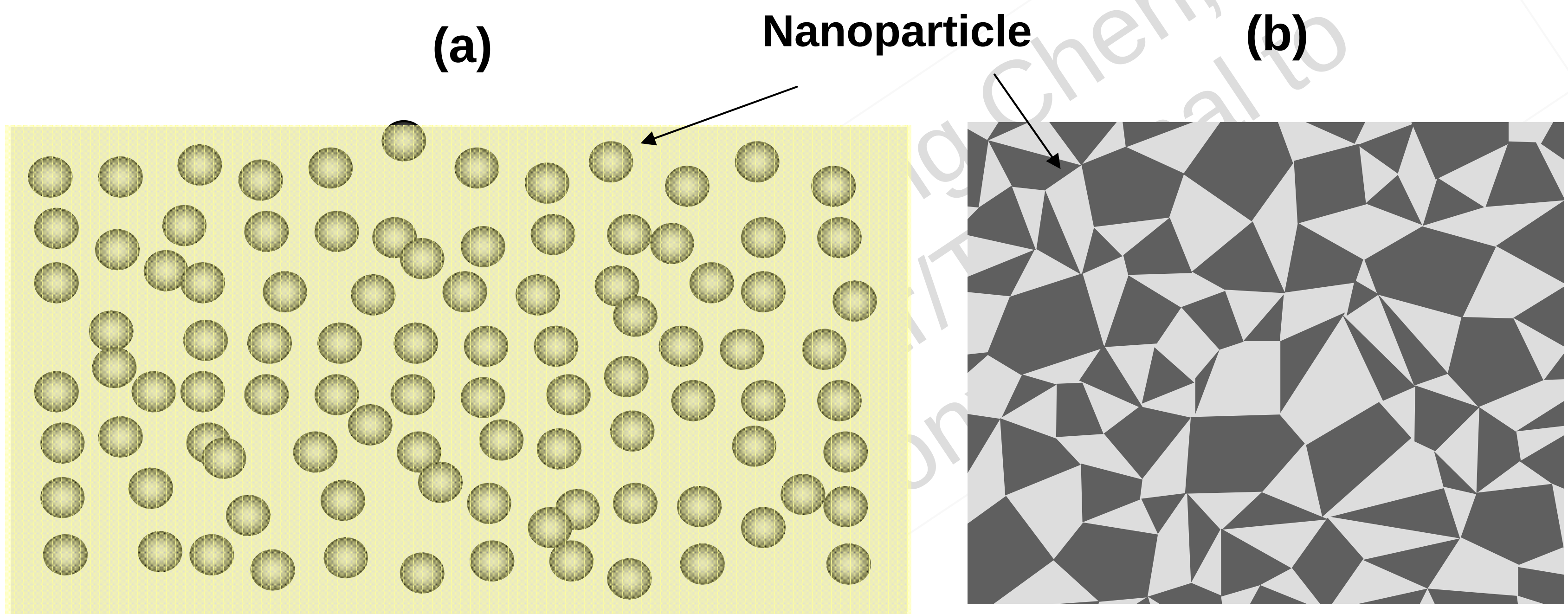

– Increase interfacial scattering by mixing nano-sized particles.

– Enable batch fabrication for large scale application.

Nanostructured Bi_2Te_3

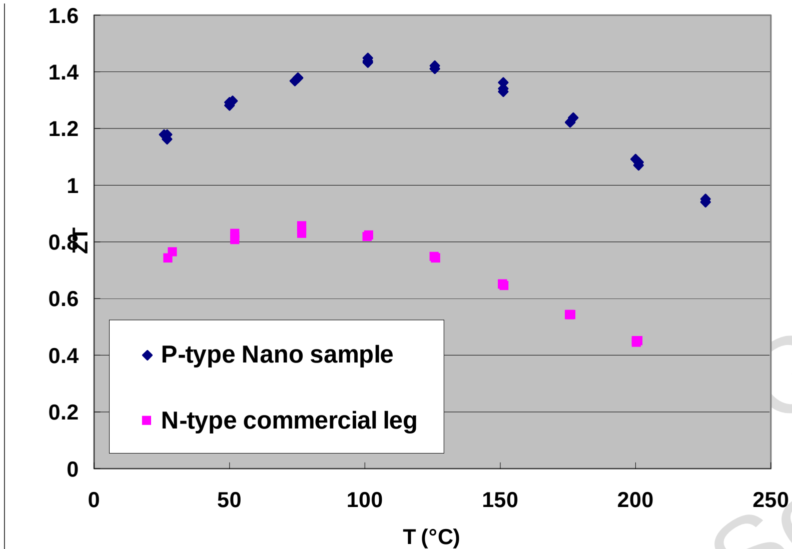

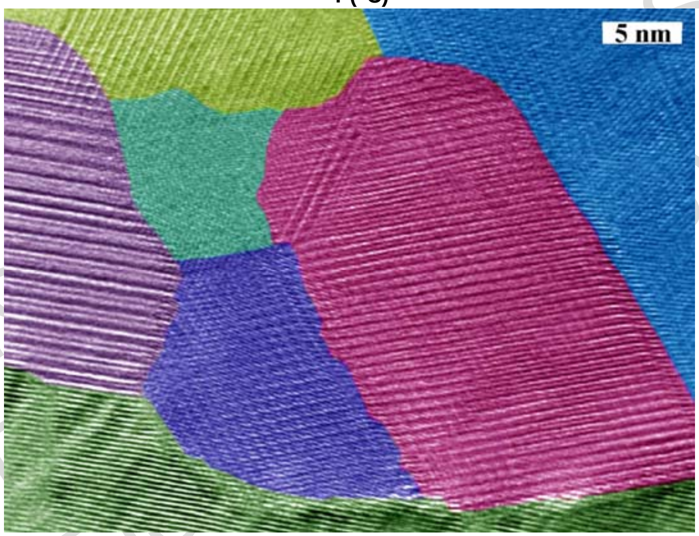

Poudel et al., Science, 320, 634, 2008

Images removed due to copyright restrictions.

Please see: Fig. 2e in Joshi, Giri, et al. "Enhanced Thermoelectric Figure of Merit in Nanostructured p-type Silicon Germanium Bulk Alloys." *Nano Letters* 8 (2008): 4670-4674.

Fig. 3d in Wang, X. W., et al. "Enhanced Thermoelectric Figure of Merit in Nanostructured n-type Silicon Germanium Bulk Alloy." *Applied Physics Letters* 93 (2008): 193121.

Thermoelectric Properties: Bi_2Te_3

$AgPb_mSbTe_{2+m}$

Images removed due to copyright restrictions.
Please see Fig. 3, 4 in Hsu, Kuei Fang, et al. "Cubic AgPbmSbTe(2+m): Bulk Thermoelectric Materialswith High Figure of Merit." *Science* 303 (February 6, 2004): 818-821.

I-V-VI$_2$ Group

$$\kappa_L = A \frac{\bar{M}\theta^3\delta}{\gamma^2 n^{2/3} T}$$

Thermal Expansion

Bulk Modulus

Molar Volume

$$\gamma = \frac{3\beta B V_m}{C_V}$$

Gruneisen Parameter

Image removed due to copyright restrictions. Please see Fig. 2 in Morelli, D. T., V. Jovovic, and J. P. Heremans. "Intrinsically Minimal Thermal Conductivity in Cubic I-V-VI2 Semiconductors." *Physical Review Letters* 101 (July 2008): 035901.

Images removed due to copyright restrictions.
Please see Fig. 1, 2, 3 in Rhyee, Jong Soo, et al. "Peierls Distortion as a Route to High Thermoelectric Performance in In4Se(3-d) Crystals." *Nature* 459 (June 18, 2009): 965-968.

Charge Density Wave

Peierls Instability

Rhyee et al., Nature, 459, 965 (2009)

Electron Quantization

<u>Quantum Well</u>

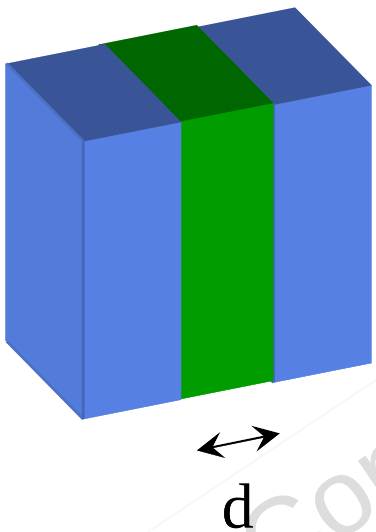

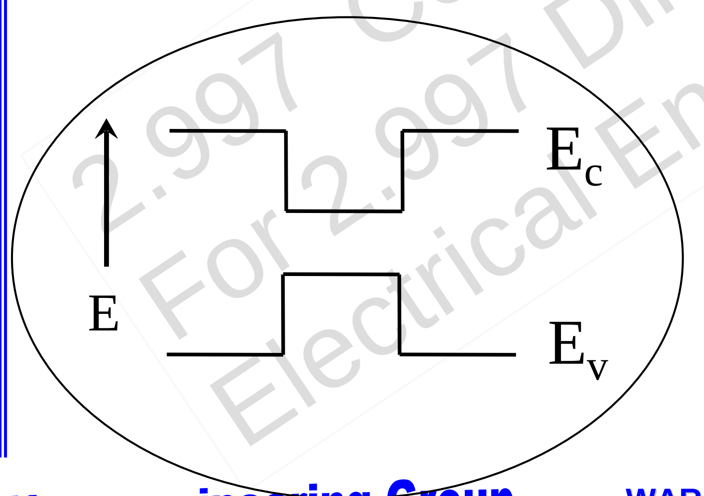

$$E = \frac{\hbar^2}{2m^*}\left[k_x^{\ 2} + k_y^{\ 2} + \left(\frac{n\pi}{d}\right)^2\right]$$

n = 1,2,3, … $k^2 = k_x^{\ 2} + k_y^{\ 2}$

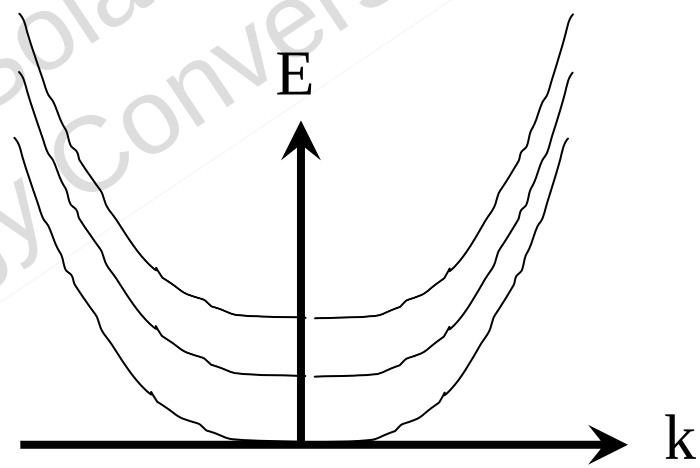

Subbands form in quantum confined directions

Density of States

$$k^2 = \frac{2mE}{\hbar^2} - \left(\frac{n\pi}{d}\right)^2$$

$$N = \sum_{-N_x/2}^{N_x/2} \sum_{-N_y/2}^{N_y/2} \sum_{n=1}^{\infty} f = \sum_{n=1}^{\infty} 2 \int_{-\pi/a}^{\pi/a} \frac{dk_x}{2\pi/L_x} \int_{-\pi/a}^{\pi/a} \frac{dk_y}{2\pi/L_y} f$$

$$= \sum_{n=1}^{\infty} \frac{A}{2\pi^2} \int_0^{\pi/a} 2\pi k dk f = \sum_{n=1}^{\infty} \frac{A}{\pi\hbar^2} \int_0^{E_a} f dE$$

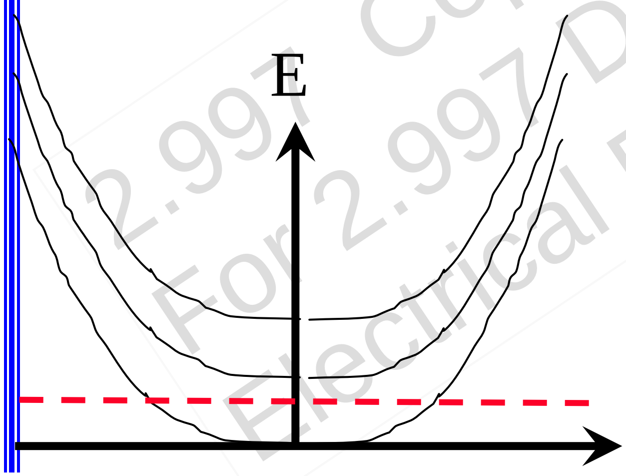

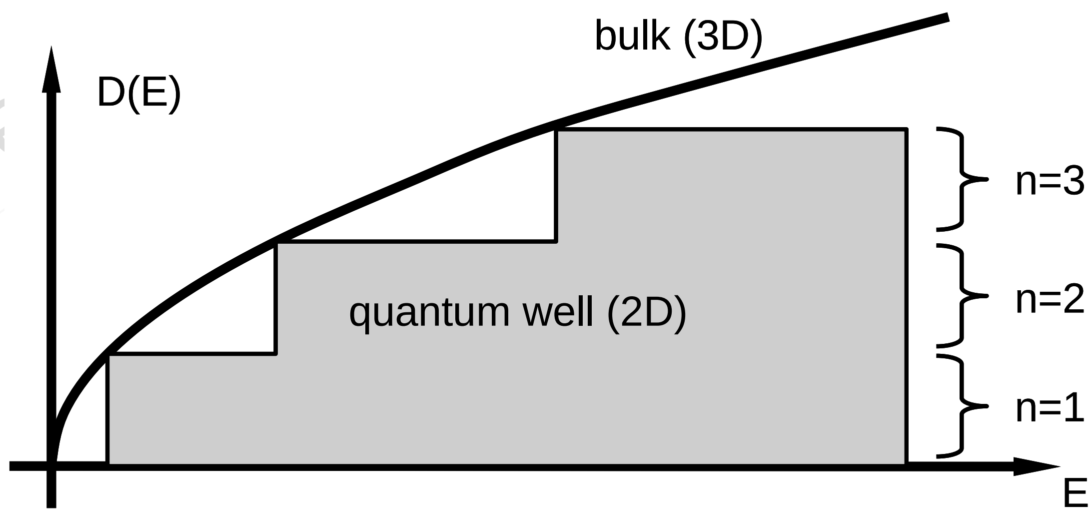

Semiconductor

$$S \propto \frac{1}{qT}\frac{\int \tau \mathbf{v}^2 D(E)(E-E_F)(-\partial f_{eq}/\partial E)dE}{\int \tau \mathbf{v}^2 D(E)(-\partial f_{eq}/\partial E)dE} \propto \langle E - E_f \rangle$$

$$\sigma \propto \int \tau \mathbf{v}^2 D(E)(-\partial f_{eq}/\partial E)dE$$

Maximize $S^2\sigma$, reducing k_e

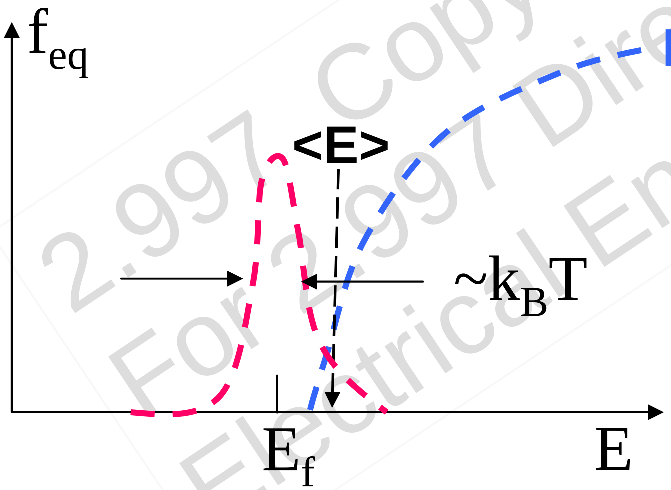

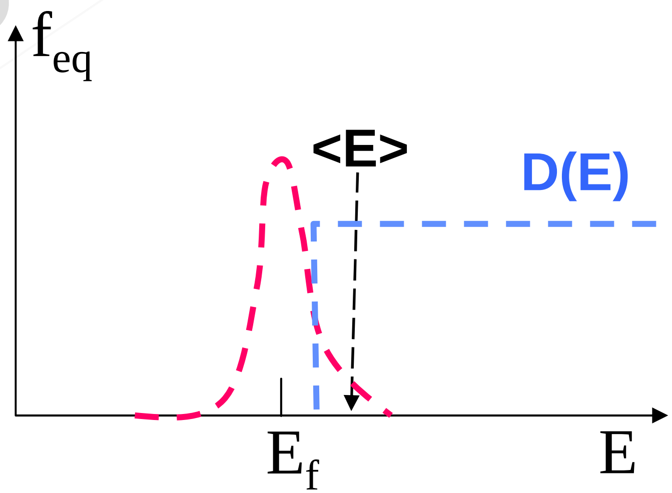

DOS of Low Dimensional Structures

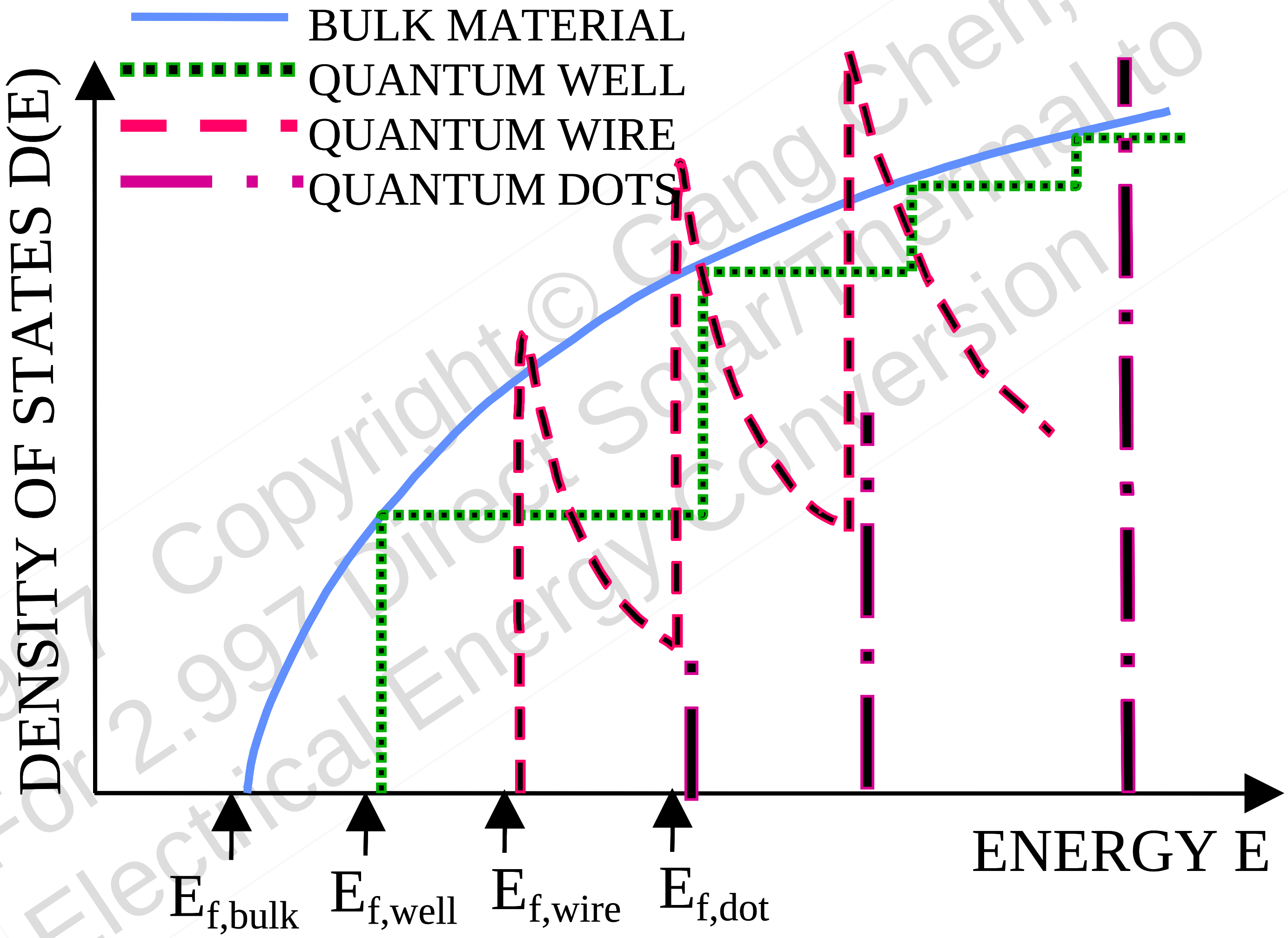

Experimental Proof of Principle

Image removed due to copyright restrictions.
Please see Fig. 1a in Hicks, L. D., et al. "Experimental Study of the Effect of Quantum-well Structures on the Thermoelectric Figure of Merit." *Physical Review B* 53 (April 1996): R10493-R10496.

Hicks and Dresselhaus (1993)

Sample Calculation

By J.S. Heremans
K_p=2 W/mK
d=2.5 nm
m*=0.15m

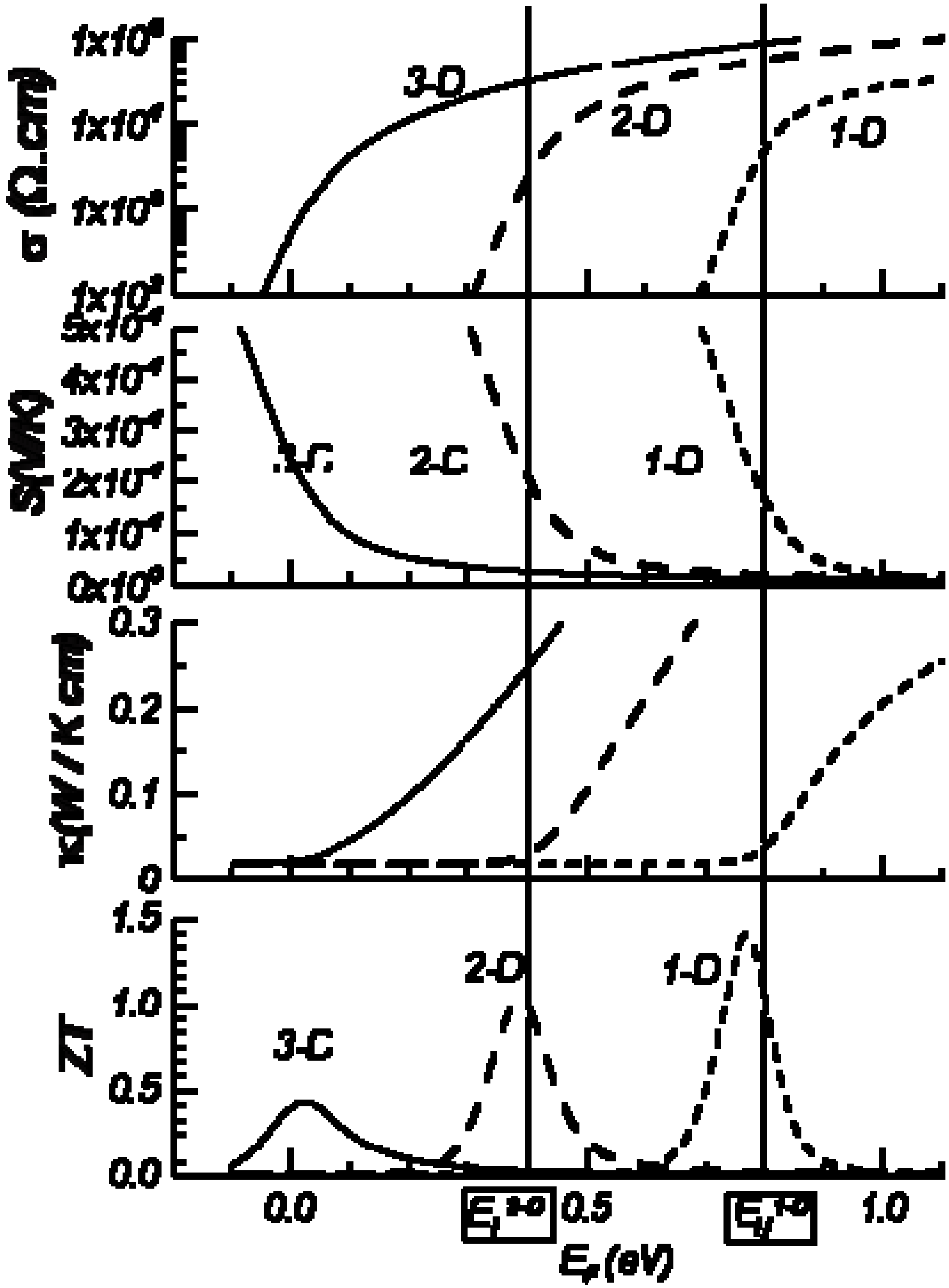

Courtesy of Joseph P. Heremans. Used with permission.

Potential Pitfalls

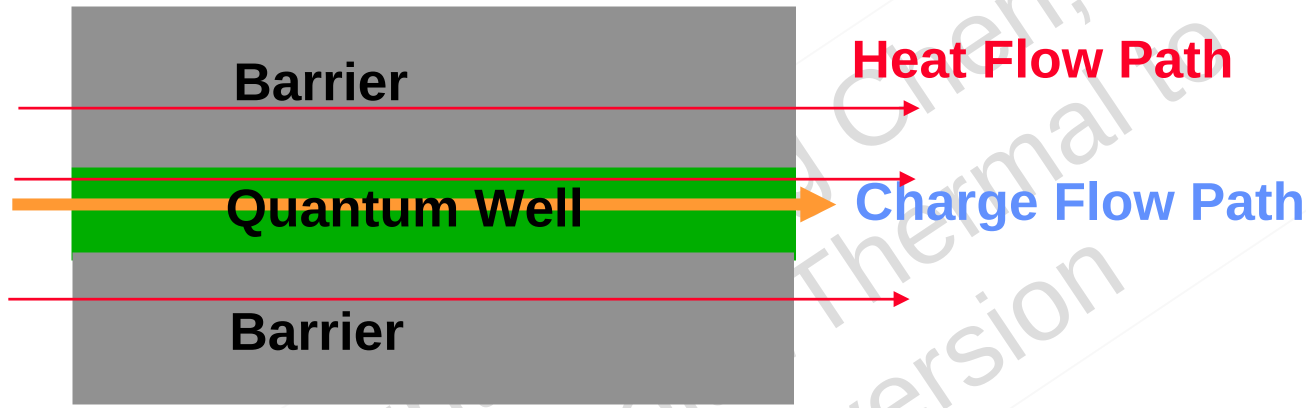

- Interface roughness scattering reducing τ
- Tunneling between layers reduces sharp DOS features

Resonant Levels

Images removed due to copyright restrictions.
Please see Fig. 1, 3 in Heremans, Joseph P., et al.
"Enhancement of Thermoelectric Efficiency in PbTe by
Distortion of the Electronic Density of States." *Science* 321 (July 2008): 554-557.

Heremans et al., Science, 321, 554 (2008)

Thermionic Emission and Energy Filtering

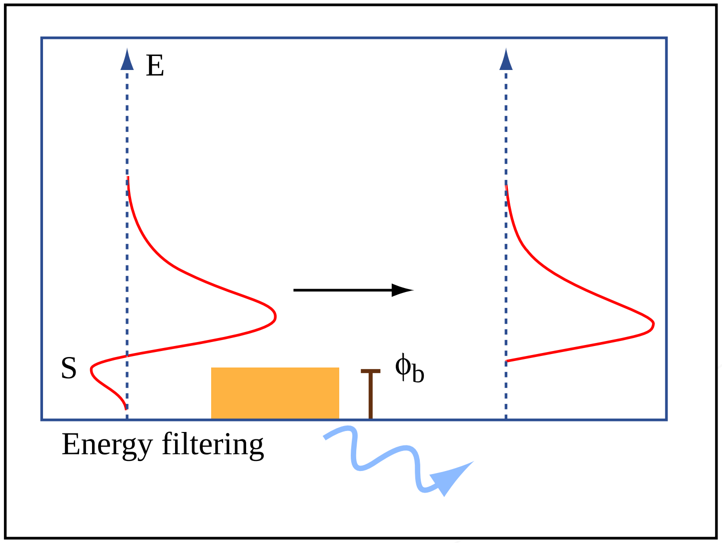

Figure by MIT OpenCourseWare.

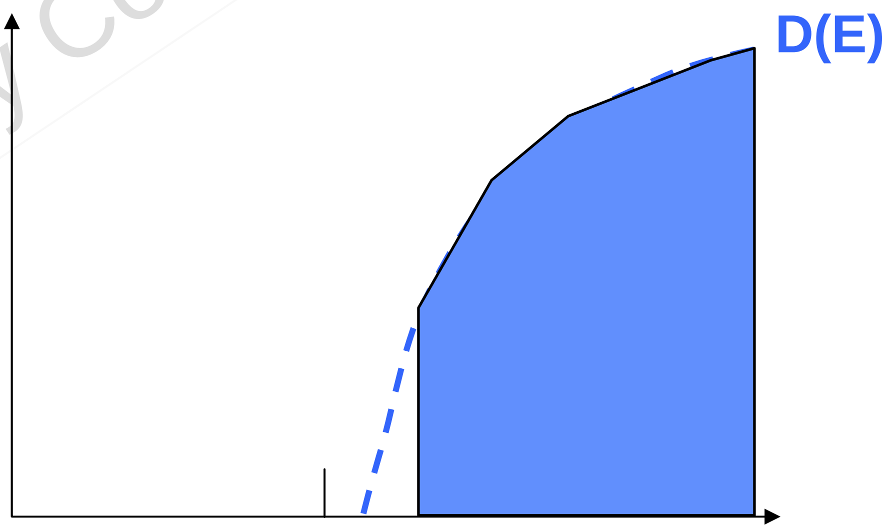

Moyzhes and Nemchinsky, Appl. Phys. Lett., 73, 1895-1897 (1998).
Shakouri and Bowers, Appl. Phys. Lett., 71, 1234 (1997).

2.997 Direct Solar/Thermal to Electrical Energy Conversion Technologies
Fall 2009